Nanoparticles

DOI: 10.1002/anie.201007731

Laser Dispersion of Detonation Nanodiamonds**

*Kai-Yang Niu, Hai-Mei Zheng, Zhi-Qing Li, Jing Yang, Jing Sun, and Xi-Wen Du**

Detonation nanodiamonds (DNDs), which were first produced from detonation of explosives in 1960s,[1] have recently found attractive applications,[2] such as in bioimaging, cellular marking, and drug delivery to DNA, thanks to their excellent biocompatibility, nontoxicity, and dimensional, thermal, and chemical stability[3]. However, it has been a challenge to deaggregate the nanodiamonds, despite many efforts during the past 40 years.[1b,4] In 2002 and 2003, Osawa et al. made significant progress by recognizing the microstructure of DNDs agglomerates and developed the technique of wet-stirred-media milling and bead-assisted sonication to destroy the agglomerant mechanically. As a result, the nanodiamonds were dispersed in solution.[1b,5] This work brought DNDs as a "novel" nanomaterial into nanoscience and bionanotechnology.[2a,3c,4,6] However, the mechanical process may contaminate the nanodiamonds,[1b,7] and the dispersity of DNDs still needs to be improved.[1b,5,8]

Laser heating has been widely adopted for the synthesis of nanomaterials.[9] Herein, we propose that selective laser heating in liquids can be an effective solution process to deaggregate DNDs. It was demonstrated that the raw DNDs are aggregates of primary nanodiamonds connected with amorphous carbon and covalent bands.[1b] On the other hand, nanodiamonds have a large band gap of about 5.5 eV and are transparent to visible or infrared light; in contrast, amorphous carbon without a band gap can absorb the light and be heated.[10] On the basis of this understanding, we suspended the DNDs in liquid and irradiated them using an infrared laser (wavelength 1064 nm). The amorphous carbon absorbs the laser energy and is heated into hot carbon species. Subsequently, the explosion of amorphous carbon can further destroy the covalent bonds between primary nanodiamonds in DNDs. As a consequence, the primary nanodiamonds are released from DNDs and dispersed in liquid free of contamination.

Once the amorphous carbon and covalent bonds are removed, the fresh surface of the primary nanodiamonds is then exposed to the liquid environment and can bond facilely with the solvent, thus giving rise to functional nanomaterials. Hu et al. reported the one-step laser synthesis of luminescent nanocomposites by in situ modification of carbon nanodots with organic molecules during nanoparticle formation.[11] Similarly, we have produced nanodiamonds with unique properties by varying the liquid medium. We find that magnetic properties of DNDs change significantly after deaggregation, and the well-dispersed nanodiamonds coated with organic ligands give visible-light emission. Because of the inert features of nanodiamonds, these luminescent nanomaterials are expected to find useful applications in bioimaging and biosensing.

Three samples were prepared to investigate the effect of different treatments on the dispersion of DNDs. Samples 1, 2, and 3 (denoted S1, S2, and S3) were the products of sonication, acid oxidization, and laser treatment of raw DNDs, respectively. The raw DNDs are severe agglomerates with amorphous carbon around the crystal nanodiamonds (Supporting Information Figure S1). After sonication treatment, the nanodiamonds in S1 were still agglomerated and coated with amorphous or graphitic carbon (Figure 1a,d). After acid oxidization, the degree of aggregation in S2 has decreased (agglomerate diameter ca. 50 nm, Figure 1b,e). However, well-dispersed nanodiamonds were only obtained in S3 after laser treatment (Figure 1c,f). TEM images indicated that the average size of the nanodiamonds is about 6.3 nm (measured from 150 particles; see inset in Figure 1c).

The suspension of nanodiamonds with fine sizes (S3) was stable even after five-month storage. In contrast, S1 and S2 precipitated completely only after one month (Supporting Information Figure S2). As a control experiment, laser irradiation of acid-oxidized DNDs did not markedly improve their dispersity (see the results for S4 in Supporting Information Figure S3).

The size distributions of the three samples subjected to different treatments (S1, S2, and S3) were measured using dynamic light scattering (DLS). The effective diameters of particles in S1, S2, and S3 are 1300, 167, and 9.8 nm, respectively (Figure 2a). Although there are deviations between the effective diameters determined by DLS and those observed in the TEM images (e.g., 9.8 vs. 6.3 nm for S3), the results from these measurements agree roughly and show the same trend. We further measured size distribution of DNDs after they were irradiated for different lengths of time. DLS results show that the extent of aggregation decreases gradually with the irradiation time, which suggests that the

[*] K. Y. Niu, Dr. J. Yang, Prof. J. Sun, Prof. Dr. X. W. Du
Tianjin Key Laboratory of Composite and Functional Materials
School of Materials Science and Engineering, Tianjin University
Tianjin 300072 (People's Republic of China)
Fax: (+86) 22-2740-5694
E-mail: xwdu@tju.edu.cn

Dr. H. M. Zheng
Materials Sciences Division, Lawrence Berkeley National Laboratory
Berkeley, CA 94720 (USA)

Prof. Z. Q. Li
School of Sciences, Tianjin University
Tianjin 300072 (People's Republic of China)

[**] This work was supported by the Specialized Research Fund for the Doctoral Program of Higher Education (Nos. 200800560050 and 20090032120024), the Natural Science Foundation of China (Nos. 50902103 and 50972102), and the National High-tech R&D Program of China (Nos. 2007AA021808 and 2009AA03Z301).

Supporting information for this article is available on the WWW under http://dx.doi.org/10.1002/anie.201007731.

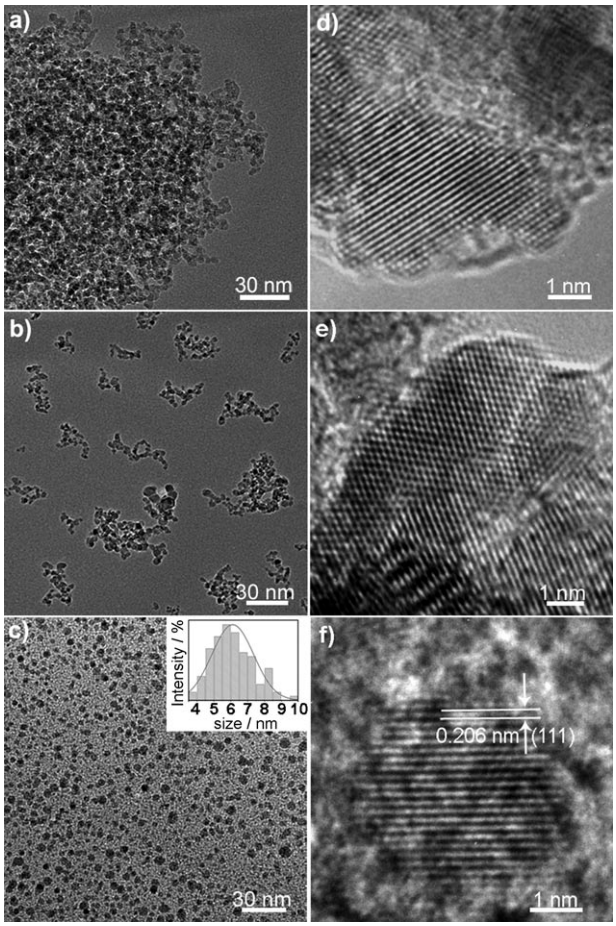

Figure 1. TEM images of a) S1, b) S2, and c) S3 and corresponding high-resolution TEM (HRTEM) images (d)–(f). The inset in (c) shows the histogram of size distribution in S3.

large aggregates experience gradual dissociation under laser irradiation (Supporting Information Figure S4). When a nanosecond pulsed laser with a wavelength of 532 nm was used to irradiate the raw DNDs, well-dispersed products could also be obtained (Supporting Information Figure S5). Therefore, this selective heating by laser irradiation is not limited to a specific laser wavelength or a specific pulse width.

XRD profiles of the three samples (S1, S2, and S3) are shown in Figure 2b. The DNDs after sonication (S1) show a broad peak at 23° corresponding to amorphous carbon.[12] This peak disappears after both acid oxidation (S2) and laser irradiation (S3). Thermogravimetric analysis (TGA, Figure 2c) indicates that the initial temperature of weight loss increases in the order of S1, S3, S2. We believe that the weight loss at low temperature is related to the existence of active amorphous carbon, and thus the three treatments have different capabilities to eliminate amorphous carbon (acid oxidization > laser irradiation > ultrasonic treatment). The fine features of TGA curves need further investigation.

We have further studied the magnetic properties of the three samples (S1, S2, and S3). To exclude the influence of ferromagnetic impurities (Fe, Co, etc.), we washed S3 with dilute nitric acid, and analysis by atomic absorption spectroscopy (AAS) confirmed the absence of ferromagnetic elements. Figure 2d shows the magnetic-field dependence of magnetization measured at room temperature. All samples reveal ferromagnetic characteristics, and the magnetization increases in the sequence of S1, S2, and S3 at a given magnetic field. Moreover, the magnetization of S1 slightly decreases with increasing magnetic field at higher field. The magnetization curve of the raw DNDs (not shown) is identical to that of S1.

It was reported that the bulk diamond and amorphous carbon possess intrinsic diamagnetic properties,[13] while the surface defects of nanodiamonds, such as dangling bonds and the sp^2 and sp^3 coordinated carbon atoms, can give rise to ferromagnetism.[14] We believe that our observed magnetization of nanodiamonds reflects the concentration of surface defects. For raw DNDs and S1 (prepared by sonication), the nanodiamond surface of is covered with covalent bonds and amorphous carbon, leaving limited dangling bonds and thus resulting in weak magnetism at low field. As the applied magnetic field increases, the diamagnetic characteristics from the diamond and amorphous carbon take over, which gives rise to the slight decrease in the magnetization (S1 in Figure 2d). In contrast, the well-dispersed nanodiamonds (S3), after being washed with dilute nitric acid to exclude impurity effects, show the largest magnetization. The higher magnetization of the completely deaggregated nanodiamonds after laser treatment can be explained by the higher concentration of surface defects. These results support the model that ferromagnetic properties of nanodiamonds arise from the surface

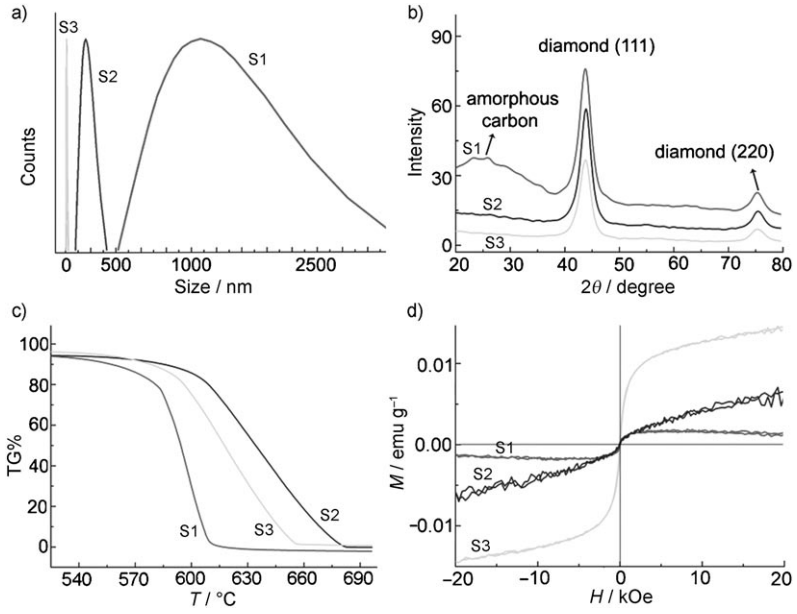

Figure 2. Characterization of the samples subjected to different treatments. a) Effective diameters of nanodiamonds measured by DLS, b) XRD profiles, c) TGA curves, and d) room-temperature magnetization versus magnetic field.

defects (such as dangling bonds) rather than from ferromagnetic impurities.

On the basis of above experiments, we propose a deaggregation mechanism of DNDs. Upon laser irradiation, DNDs agglomerates experience selective heating. As shown in Scheme 1, the primary nanodiamonds are transparent to

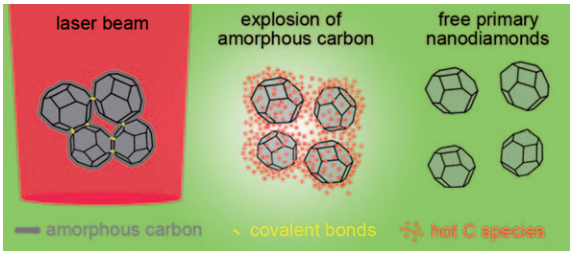

Scheme 1. Deaggregation of DNDs by laser irradiation in liquid.

the laser owing to the band gap of 5.5 eV, while the amorphous carbon can absorb the laser energy. Thus, the amorphous carbon can be heated and finally destroyed at high temperature. The fiercely exploded carbon species could further destroy the covalent bonds between the primary nanodiamonds. The carbon species react with the solution (i.e., $C + H_2O \rightarrow CO + H_2$) and escape as gases. The elimination of amorphous carbon and the breaking of covalent bonds between primary nanodiamonds leads to the well-dispersed nanodiamonds in solution. However, the amorphous carbon and covalent bonds between nanodiamonds are too strong to be destroyed by sonication alone. Although acid oxidation can remove amorphous carbon, it cannot break the covalent bonds between nanodiamonds. Therefore, the diamonds remain aggregated after sonication (S1) and acid oxidation (S2). This mechanism of selective laser heating was further confirmed by S4, for which the amorphous carbon is removed by acid oxidation,[1b] after which deaggregation by laser irradiation is no longer effective.

Deaggregation of DNDs can be carried out in different solvents, such as PEG200 (S5; PEG = poly(ethylene glycol)), methacrylic acid, and *n*-hexane (Supporting Information Figure S6). Notably, the dispersed nanodiamonds aggregated rapidly in nonpolar solvents (e.g., *n*-hexane); in contrast, they dispersed well in polar solvents such as water and ethanol. This behavior may be ascribed to the polarity of the nanodiamond surface.

After the removal of amorphous carbon and covalent bonds, the clean surfaces of primary nanodiamonds react with the surrounding molecules. Therefore, in situ surface modification is expected to occur during the laser ablation process. We have further studied the optical properties of the nanodiamonds after surface modification with different ligands.

The surface structure of the laser-treated nanodiamonds was examined by IR spectroscopy. Figure 3a shows Fourier transform IR (FTIR) spectra of raw DNDs, the nanodiamonds deaggregated by laser irradiation in water (S3), and those dispersed in PEG200 (S5). The nanodiamonds in all three samples show carboxy groups on the surface ($\nu_{C=O}$ and ν_{OH}). In contrast, the hydroxy peak at 1380 cm^{-1} (δ_{C-OH})

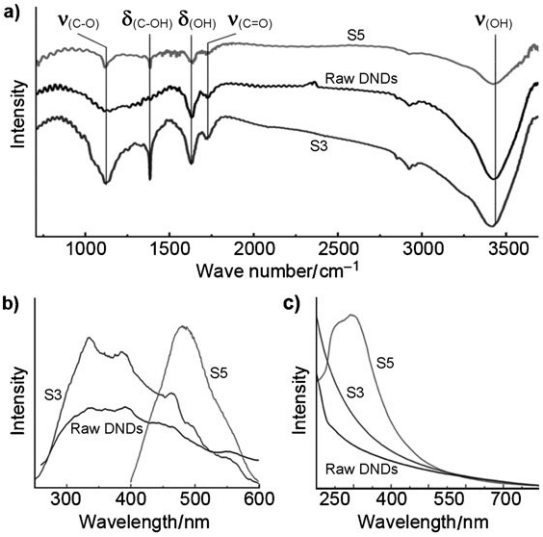

Figure 3. a) FTIR spectra of raw DNDs, S3, and S5. b) PL spectra of the raw DNDs, S3, and S5 excited by irradiation at 210 (raw DNDs, S3) and 390 nm (S5). c) Absorbance spectra of the raw DNDs, S3, and S5.

varies with the treatment process. Strong hydroxy peaks can be found from S3 and S5, while this peak is absent in raw DNDs, thus indicating that the nanodiamonds can be simultaneously functionalized when they are dispersed in liquids.

Accordingly, we compared the photoluminescence (PL) properties of the above three samples. Considering the large band gap (5.5 eV) of nanodiamonds, we excited raw DNDs with incident photons of 5.9 eV (210 nm). The PL spectrum in Figure 3b shows a very wide band in the wavelength range 200–600 nm, while the absorption spectrum of raw DNDs exhibits (Figure 3c) continuous absorption at 200–800 nm. The PL and absorption spectra of S3 show similar features to those of raw DNDs. Moreover, neither raw DNDs nor S3 can emit visible light when they are excited with lower energy light (e.g., 390 nm). However, the dispersed nanodiamonds in PEG200 (S5) show a narrow PL peak at 480 nm, which is distinctly different from that of pure PEG200 (PL band around 440 nm, Supporting Information Figure S7a). S5 also has a strong absorption peak at 300 nm (Figure 3c), thus indicating the absorption of PEG molecules on the nanodiamond surface. Moreover, weak up-conversion photoluminescence can be obtained from S5, that is, PL bands centered at 475 and 495 nm were detected when 580 and 600 nm irradiation was used (Supporting Information Figure S7b), which might be a universal feature of the nanodiamonds.

Combining the FTIR results with PL and absorption spectra, we conclude that the solvent media for laser irradiation can influence the surface chemistry and the optical properties of the products remarkably. Raw DNDs contain mainly C=O and C=C bonds at the surface. However, additional C–OH bonds are created on the surface of DNDs after they are dispersed in water and PEG200. The C–OH bonds alone in S3 cannot change PL properties; however, PEG200 ligands on the DND surface (S5) can

significantly improve the visible-light emission. Our results are consistent with the mechanisms proposed in previous studies, namely, that the surface states play a key role in determining the optical properties.[10,15]

In summary, detonation nanodiamonds were deaggregated by laser irradiation in liquid. The amorphous carbon could absorb the laser energy and be heated, but the primary nanodiamonds are transparent to the laser. The explosion of amorphous carbon further destroys the covalent bonds between primary nanodiamonds and thereby releases the nanodiamonds. The deaggregated nanodiamonds (ca. 6.3 nm diameter) were well-dispersed and stable in many nonpolar solvents. The surface of nanodiamonds could be modified by the solvent molecules during laser ablation, which endows the nanodiamonds with visible-light emission.

Experimental Section

Raw DNDs and other reagents were purchased from Jiangtian Chemical Technology Corporation, China. S1 was obtained by sonicating raw DNDs (10 mg) in deionized water (30 mL) for 1 h. To prepare S2, DNDs (500 mg) were dispersed in a mixture of sulfuric acid (98%) and nitric acid (70%; 3:1 v/v, 100 mL). The mixture was heated at reflux (75 °C) for 72 h and then centrifuged and washed with deionized water; finally the DNDs were dried at 100 °C for 48 h. S2 was then obtained by dispersing the acid-oxidized DNDs (10 mg) in deionized water (30 mL).

For the laser irradiation treatment, the raw DNDs were first suspended in liquid under sonication, then they were irradiated by a Nd:YAG laser (1064 nm). The laser beam was focused on the liquid surface with a spot size of 0.2 mm (see Supporting Information Figure S8). The laser pulse width, frequency, and single-pulse energy were set to 1 ms, 30 Hz, and 1.8 J, respectively. All the laser ablation experiments were performed at ambient temperature and pressure. S3 was obtained by laser irradiation of raw DNDs (10 mg) in deionized water (30 mL) for 1 h. In control experiments, S4 was prepared by laser ablation of S2 for 1 h under the same conditions as for S3, S5 was obtained by irradiation of raw DNDs (10 mg) in 30 mL poly(ethylene glycol) 200 (PEG200) for 1 h.

The morphology and structure of the samples were characterized using a Rigaku D/max 2500v/pc X-ray diffractometer and an FEI Technai G2 F20 transmission electron microscope with a field emission gun. The size distribution was measured by dynamic light scattering (DLS) at 25 °C in ethanol with a Brookhaven Zetasizer (Brookhaven Instruments Ltd., U.S.). Thermogravimetric analysis was carried out in a Pyris TGA7 thermogravimeter (Perkin–Elmer Corporation). For the measurement of magnetic properties, samples were washed with dilute nitric acid (1%) at room temperature for 48 h and then with deionized water five times, dried at 80 °C for 24 h, and measured using a vibrating sample magnetometer equipped with a physical properties measurement system (PPMS-6000, Quantum Design). Ferromagnetic elements were identified using a GRN1-WFX-130 atomic absorption spectrophotometer. The above dried samples were dispersed in ethanol for the photoluminescence and absorption measurements using a Hitachi F-4500 fluorescence spectrometer and a Hitachi U-3010 UV/Vis spectrometer, respectively. The infrared spectra were measured with a Thermo Nicolet Nexus 470 FTIR Spectrophotometer.

Received: December 9, 2010
Published online: April 7, 2011

Keywords: dispersion · laser chemistry · nanoparticles · surface chemistry

[1] a) N. R. Gneiner, D. S. Phillips, J. D. Johnson, J. Volk, *Nat. Mater.* **1988**, *333*, 440; b) E. Ōsawa, *Pure Appl. Chem.* **2008**, *80*, 1365.
[2] a) A. M. Schrand, S. A. C. Hens, O. A. Shenderova, *Crit. Rev. Solid State Mater. Sci.* **2009**, *34*, 18; b) I. P. Chang, K. C. Hwang, C. S. Chiang, *J. Am. Chem. Soc.* **2008**, *130*, 15476; c) H. Huang, E. Pierstorff, E. Osawa, D. Ho, *Nano Lett.* **2007**, *7*, 3305; d) J. I. Chao, E. Perevedentseva, P. H. Chung, K. K. Liu, C. Y. Cheng, C. C. Chang, C. L. Cheng, *Biophys. J.* **2007**, *93*, 2199.
[3] a) J. Y. Raty, G. Galli, *Nat. Mater.* **2003**, *2*, 792; b) A. M. Schrand, H. J. Huang, C. Carlson, J. J. Schlager, E. Osawa, S. M. Hussain, L. M. Dai, *J. Phys. Chem. B* **2007**, *111*, 2; c) A. Krueger, *Chem. Eur. J.* **2008**, *14*, 1382.
[4] A. Krueger, *J. Mater. Chem.* **2008**, *18*, 1485.
[5] M. Ozawa, M. Inaguma, M. Takahashi, F. Kataoka, A. Kruger, E. Osawa, *Adv. Mater.* **2007**, *19*, 1201.
[6] A. Krueger, *Adv. Mater.* **2008**, *20*, 2445.
[7] J. S. Tse, D. D. Klug, F. M. Gao, *Phys. Rev. B* **2006**, *73*, 142102.
[8] K. Iakoubovskii, K. Mitsuishi, K. Furuya, *Nanotechnology* **2008**, *19*, 155705.
[9] a) G. W. Yang, *Prog. Mater. Sci.* **2007**, *52*, 648; b) V. Amendola, M. Meneghetti, *Phys. Chem. Chem. Phys.* **2009**, *11*, 3805; c) P. Liu, H. Cui, C. X. Wang, G. W. Yang, *Phys. Chem. Chem. Phys.* **2010**, *12*, 3942.
[10] J. Sun, S. L. Hu, X. W. Du, Y. W. Lei, L. Jiang, *Appl. Phys. Lett.* **2006**, *89*, 0.
[11] S. L. Hu, K. Y. Niu, J. Sun, J. Yang, N. Q. Zhao, X. W. Du, *J. Mater. Chem.* **2009**, *19*, 484.
[12] M. Noh, Y. Kwon, H. Lee, J. Cho, Y. Kim, M. G. Kim, *Chem. Mater.* **2005**, *17*, 1926.
[13] J. Heremans, C. H. Olk, D. T. Morelli, *Phys. Rev. B* **1994**, *49*, 15122.
[14] a) T. L. Makarova in *Progress in Industrial Mathematics at Ecmi 2006*, *Vol. 2* (Eds.: L. L. Bonilla, M. Moscoso, G. Platero, J. M. Vega), VCH, Berlin, **2008**, p. 467; b) S. Talapatra, T. Kim, B. Q. Wei, S. Kar, R. Vajtai, G. V. S. Sastry, M. Shima, Srivastava, D. P. M. Ajayan, *Nanopages* **2006**, *1*, 315; c) T. Enoki, Y. Kobayashi, C. Katsuyama, V. Y. Osipov, M. V. Baidakova, K. Takai, K. I. Fukui, A. Y. Vul, *Diamond Relat. Mater.* **2007**, *16*, 2029.
[15] V. N. Mochalin, Y. Gogotsi, *J. Am. Chem. Soc.* **2009**, *131*, 4594.

